Probe for measuring ultrasonic fields using short in-fibre Bragg gratings

NE Fisher, DJ Webb, CN Pannell, DA Jackson[a], LR Gavrilov , JW Hand[b], L Zhang and I Bennion[c]

[a]Applied Optics Group, The University, Canterbury, Kent, CT2 7NR, UK
Tel: (+44) 1227 764000, Fax: (+44) 1227 827558
[b]Radiological Sciences Unit, Hammersmith Hospital, Du Cane Road, London, W12 OHS, UK
[c]Photonics Research Group, Department of Electronic Engineering, Aston University, Birmingham, B4 7ET, UK

ABSTRACT

We demonstrate that short in-fibre Bragg gratings (with a length less than the acoustic wavelength in fused quartz) coupled with an appropriate desensitisation of the fibre, may be successfully used to measure MHz ultrasonic fields.

Keywords: Bragg grating, ultrasound, acoustic, medical

1. INTRODUCTION

There is a need for the assessment of the safety of ultrasound for medical applications[1,2,3] due to the trend towards increasing output powers from diagnostic ultrasound equipment and the widening use of high intensity ultrasonic fields in a range of therapeutic applications. Often the assessment of such fields is based upon theoretical models of some complexity and so a direct determination of them *in vivo* is of importance. Conventional detection is most commonly achieved using piezoelectric devices but suffers from a susceptibility to electromagnetic interference and signal distortion. To overcome these "electrical" problems several approaches utilising optical fibres based on interferometric or polarimetric techniques have been described[4,5,6,7].

In this paper we demonstrate that in-fibre Bragg gratings (FBGs) may also be used to detect high frequency (MHz) ultrasonic fields. These devices offer distinct advantages such as ease of multiplexing, simultaneous measurement of temperature, and a potentially low cost[8,9]. We found however, that the acoustic coupling from the ultrasonic field to the grating leads to the formation of standing waves in the fibre. Because of these standing waves, the system response is complex and, as we show, the grating does not act as an effective probe. However, significant improvement in its performance may be gained using short gratings coupled with appropriate desensitisation of the fibre.

2. EXPERIMENT

The arrangement used to interrogate the grating is shown in figure 1. This utilised a ramped lithium niobate phase modulator (closely set to produce a 2π peak-to-peak phase excursion) to frequency shift the light in one arm of an unbalanced Mach-Zehnder interferometer (MZ) and thus allowed the use of heterodyne signal processing[10,11]. Light from a pig-tailed superluminescent diode (*Superlum*, Moscow) giving an output power of 1mW centred at 824nm with a bandwidth of ≈42nm was launched into the unbalanced MZ; hence a channelled spectrum was created at the interferometer's outputs which was incident on the grating. Incorporated in one arm of the MZ was the phase modulator. The other arm contained a variable air gap which allowed the optical path difference (OPD) between the two arms to be adjusted. Provided that the OPD between the MZ's arms is longer than the source coherence length and shorter than the effective coherence length of the back-reflected light from the grating, interference signals are observed at the detector which can be expressed as

SPIE Vol. 3555 • 0277-786X/98/$10.00

$$I(\lambda_B) = A(1 + V\cos[\omega' t + \Phi + \delta\Phi \sin\omega t + \phi(t)]) \quad (1)$$

Here, λ_B is the wavelength of the reflected light from the modulated grating, ω' is the angular frequency of the ramp modulation, A is proportional to the grating reflectivity, V is the visibility of the signals (dependent on the grating bandwidth and the polarisation properties of the system), $\Phi = 2\pi.OPD/\lambda_B$ and $\phi(t)$ is a random phase drift term. A sinusoidally strain-induced change in λ_B from the grating - ($\delta\lambda_B$) - induces a change in phase shift in equation 1, given by

$$\delta\Phi \sin\omega t = [2\pi.OPD/\lambda_B{}^2].\ [\delta\lambda_B] \sin\omega t \quad (2)$$

where ω is the angular frequency of the ultrasound incident on the grating. Hence, from equation 1, strain induced changes in λ_B induce a corresponding phase modulation of the electrical carrier produced by the phase modulator, which we measured by determining the amplitudes of the resulting upper and lower side-band frequency components observed on a radio frequency spectrum analyser.

The sensitivity of the system was determined by two competing effects. From equation 2, an increase in OPD will result in a proportional increase in the amplitude of the phase modulation. On the other hand, increasing the OPD beyond the coherence length of the light reflected by the grating will result in a reduction in the visibility and hence the height of the carrier and side-bands. In practice, the sensitivity was optimised by adjusting the OPD to obtain the maximum side-band amplitude.

The phase modulator was ramped at, and hence generated a carrier signal at, 10MHz. The grating we used had a nominal Bragg wavelength of 820nm, a bandwidth of 0.2nm, a reflectivity of 80% and a length of 5mm. The transducer was driven (in water) in continuous mode via a RF amplifier (model ENI 240L, Electronic Navigation Industries, New York) and generated a maximum acoustic pressure of ≈2Atm (measured using a PVDF membrane hydrophone calibrated by the *National Physical Laboratory, Teddington, Middx., U.K.*) in a focal spot of radius 0.114cm. This pressure corresponds to an acoustic intensity of ≈1.3 Wcm^{-2}.

3. RESULTS AND DISCUSSION

3.1. 5mm grating

In our preliminary experiments we observed two striking anomalies in the response of the system to the ultrasound. Consider figure 2 which shows a spectrum analyser trace recorded in a typical experiment. Firstly, note that the upper and lower side-band frequency components are asymmetric, and secondly note the existance of a large homodyne signal at 1.91MHz, which was up to several dB's greater than the side-band magnitudes. In this interferometric arrangement, both the homodyne signal and the asymmetry in the side-band magnitudes are unexpected system responses.

Consider also the following figures: figure 3 shows the profiles obtained by scanning the focal spot of the acoustical field longitudinally along the fibre/grating and recording one of the side-band powers (normalised by its corresponding carrier signal power) with displacement, and figures 4 and 5 which again show profiles of longitudinal scans although here we recorded the homodyne response to the acoustical field (similar profiles were also observed for the side-band powers). In both the latter cases we used the same grating but with, in each instance, different inter-acrylic jacket separations. In figure 4 the separation was ≈ 1cm and in figure 5 the separation was ≈ 6cm.

Note, in all cases, the multiple "peaks" and "troughs" in the system response which are observed over a distance that is much greater than the grating length and which can (as in the case of figure 5) extend many cms. These also are unexpected results since the radius of the focal spot is only about 1mm. However, consider the average distance between the peak responses which is 1.48mm. If we hypothesise that the acoustic coupling from the ultrasonic field to the optical fibre leads to the formation of stationary waves in the fibre (most likely due to partial back-reflections from the acrylic jacket/optical fibre boundary), this value leads to an experimental acoustic wavelength of 2.96mm which is close to the predicted value of 3.09mm for compressional waves at 1.91MHz in fused quartz. We repeated these experiments but now driving the transducer at 1.6MHz and found an experimental value of 3.76mm which is again close to the predicted value of 3.68mm. Using the same system, we then modulated the grating with low frequency (100Hz) sound waves in air and

higher frequency (76kHz) sound waves in water. In both these cases, the system response was as originally expected, with symmetric side-bands and no homodyne signal observed.

Hence we conclude the following. Compressional standing waves which can extend many cms are set up by the ultrasound in the fibre (although, as evidenced by figures 4 and 5, the acrylic jackets which are on either side of the grating do tend to attenuate the acoustic modes). These give rise to periodic maximum and minimum longitudinal displacements at the region of the grating as the acoustic focal spot is moved along the fibre which we observed as the "peaks" and "troughs" in the system response. In addition, since these waves must only partially modulate the grating (as their length is less than the grating length), this means that the grating is subject to a *non-uniform* strain; sections of the grating will be unmodulated, and other modulated sections will be out of phase with each other. The FBG now behaves in a manner similar to that of smaller separate gratings which are adjacent to each other, each of which back-reflects light of slightly different wavelengths. The result is that various regions of the grating will act as spectral filters for the back-reflected light from other regions of the grating and so give rise to amplitude modulations (this is analagous to sensing schemes where a reading grating is used to convert a modulated wavelength shift from a sensing grating into an amplitude modulation[8]). To validate this, we shone light directly onto the FBG (via a coupler), without the interferometer present, and observed a signal at 1.91MHz (plus additional smaller harmonics). Hence, the homodyne signal observed using the interferometric scheme stems from an amplitude variation with, in this case, a measured modulation depth of a few per cent.

To model what effect an amplitude modulation would have on the interferometric signals, the constant A in equation 1 may now be replaced (in the simplest case) with $A[(1-b) + b\cos(\omega t + \varphi)]$ where b is a modulation index and φ is a phase term. As we showed in reference 12, solving for the frequency spectra for this modified variant of equation 1 leads to an asymmetry in the side-band magnitudes, as observed in experiment.

We finally note that the wavelength of the lower frequency sound is greater than the length of the grating, hence in these cases the grating was subject to a more uniform strain and so none of the anomalies in the system response were observed.

3.2. 1mm grating

Based on our hypothesis, it is apparent that for the grating to operate correctly in response to the MHz acoustic field, the grating length should be made smaller than half the acoustic wavelength in fused quartz. In order to demonstrate this, we took a standard 5mm grating and gradually removed small pieces of it from one end until approximately only 1mm of grating was remaining. As each piece was removed, we recorded the system response to the ultrasonic field using the shortened grating, and noted a dramatic decrease in the homodyne signal along with more symmetric side-band magnitudes.

However because of the results of figure 3, 4 and 5, it is apparent that this shortened grating on its own cannot be used as a high frequency probe since it will exhibit insufficient longitudinal resolution. In order to obtain an improved performance we must first desensitise nearly all the fibre to the acoustical field. This we did by jacketing the fibre with PVC sleeving (diameter < 1mm) such that only the 1mm grating at the end of the fibre was exposed to the field. The results of a longitudinal scan and a lateral scan of the acoustical focal spot are shown in figures 6 and 7, respectively. As may be seen, these data compare favourably with the diameter of the main diffraction maximum of the transducer.

We finally show in figure 8 the detected magnitude of one of the side-bands (normalised by its corresponding carrier signal) as a function of acoustical pressure incident on the grating. It is clear that the system response is linear and (for this probe) we determined a noise limited pressure resolution of $\approx 4.5 \times 10^{-3}$ Atm / $\sqrt{\text{Hz}}$ which corresponds to a noise-limited intensity resolution of about 1×10^{-3} Wcm^{-2} $\text{Hz}^{-1/2}$.

4. GENERAL DISCUSSION

The improvement in the system response using a short grating is significant. However, several points should be noted.

Firstly, in our experiment, by shortening the grating we have dramatically reduced its reflectivity (in this case by a factor of well over 100) as well as increased its bandwidth, and so limited its noise-limited resolution. For applications involving high power ablation where pulsed ultrasound intensities can be several or even thousands Wcm^{-2}, the resolution we

obtained is sufficient. For physiotherapy treatments where the acoustic intensities may vary from about 0.2 to 2 Wcm^{-2}, an improvement will be necessary. Gratings, however, of lengths less than 1mm but with 90% reflectivity have been manufactured and so we anticipate a greatly improved pressure resolution using such gratings.

Secondly, based on the stationary wave model, a limiting factor in the successful performance of the grating is that its length should be less than half the acoustic wavelength in fused quartz. This sets an upper limit on the incident acoustic frequency which can be measured. Fortunately, frequencies of between 500kHz and 4MHz are generally used in most medical applications of ultrasound which implies that the grating lengths should be no greater than about 0.5mm for the highest frequency. Again, such lengths are available. In the case of lithotripsy, multiple frequency components may be generated. However, as the acoustic field traverses several cms of tissue, the higher order modes are in general significantly attenuated. Hence, in certain cases, acoustic fields of only a few MHz may be of importance.

An unrelated point entails the grating acting as an acoustic probe in "smart structure" design. Here acoustic emission is monitored and gives information about twinning, dislocation motion, cracking etc. in the material[13]. Of course, the response of the grating to multi-frequency bursts needs to be investigated. However, typical frequency spectra ranges from about 0.1 to 1.0MHz and so readily available gratings of lengths 1 to 2mm may (in principle) be used.

Thirdly, more sophisticated techniques (entailing multiple coatings) for desensitising optical fibres have been reported[14]: in our experiments we observed fluctuations in the R.F. power (to the transducer) as the FBG sensor was moved around in the vicinity of the focal spot. This was especially evident when the focal spot was incident on the PVC sleeving and is evidence for back-reflections and scattering of the acoustical field by the sensor. Obviously, reducing the dimensions of the shielding by using these multiple coatings could greatly minimise this scattering. In addition, it is worth mentioning that if the acoustic modes in the fibre can be significantly attenuated using multiple coatings (as we found using the sleeving[12]) then in principle it should be possible to multiplex FBGs on to the same fibre with little or no "acoustic cross-talk" between them.

Finally, as far as we are aware, this is the first time that data indicating the presence of acoustic stationary waves in the fibre, have been reported. Because the FBG sensor is localised in the fibre, we can see evidence for this in our longitudinal scans. In some other interferometric and polarimetric schemes, the sensing element is the entire fibre length. Sensing is therefore not localised and so in performing longitudinal scans, evidence for the stationary waves may not be readily observable.

5. CONCLUSIONS

We have demonstrated that a Bragg grating may function effectively as a point ultrasonic probe with mm resolution if: (a) the grating length is small (less than half the acoustic wavelength in fused quartz) and (b) the fibre is appropriately desensitised. A distinct advantage this probe has over some other optical sensors is its potential to also measure simultaneously temperature. This is a critical factor in hyperthermia treatments where the temperature distribution in tumors needs to be monitored. Schemes using FBGs for temperature measurements only in such applications have been well demonstrated[9], and we have recently carried out preliminary research to investigate the simultaneous recovery of temperature and ultrasonic field[15].

6. REFERENCES

1. WL Nyborg, "Optimization of exposure conditions for medical ultrasound", *Ultrasound Med. Biol.* **11**, pp. 245-260. 1985
2. NCRP, "Biological effects of ultrasound: mechanisms and clinical implications", report 74 of the National Council of Radiation Protection and Measurements. 1983
3. CR Hill, "Optimum acoustic frequency for focused ultrasound surgery", *Ultrasound Med. Biol.* **20**, pp. 271-277. 1994
4. RP De Paula, L Flax, JH Cole and JA Bucaro, "Single mode fiber ultrasonic sensor", *IEEE J. Quant. Electron.* **18**, pp. 680-693. 1982
5. HLW Chan, KS Chiang, DC Price and JL Gardener, "The characterisation of high frequency ultrasonic fields using polarimetric optical fiber sensor" *J. Appl. Phys.* **66**, pp. 1565-1570. 1989

6. S Knudsen and S Blotekjaer, "An ultrasonic fiber-optic hydrophone incorporating a push-pull Sagnac interferometer", *J. Lightwave Technol.* **12**, pp. 1696-700. 1994
7. PC Beard and TN Mills, "Miniature optical fibre ultrasonic hydrophone using a Fabry-Perot polymer film interferometer", *Electr. Lett.* **33**, pp.801-803. 1997
8. Y-J Rao, "In-fibre Bragg grating sensors", *Meas. Sci. Technol.* **8**, pp. 355-375. 1997
9. Y-J Rao, DJ Webb, DA Jackson, L Zhang, and I Bennion, "In-fibre Bragg-grating temperature sensor system for medical applications", *J. Lightwave Techn.* **15**, pp. 779-785. 1997
10. DA Jackson, AD Kersey, M Corke and JDC Jones, "Pseudo-heterodyne detection scheme for optical interferometer", *Electron. Lett.* **18**, pp. 1081-1083. 1982
11 AD Kersey, TA Berkoff and WW Morey, "Fiber-optic grating strain sensor with drift-compensated high-resolution interferometric wavelength-shift detection", *Opt. Lett.* **18**, pp. 72-74. 1993
12. NE Fisher, SF O'Neill, DJ Webb, CN Pannell, DA Jackson, LR Gavrilov, JW Hand, L Zhang and I Bennion, "Response of in-fibre Bragg gratings to focused ultrasonic fields", *Proc. of 12th Int. Conf. on Optical Fiber Sens.* **16**, pp. 190-193. 1997
13. J Kaiser, "Investigation of Acoustic Emission in Tensile Testing", Ph.D thesis Technische Hochscule Munich Germany. 1950
14. N Lagakos, G KU, J Jarzynski, JH Cole and JA Bucaro, "Desensitization of the ultrasonic response of single-mode fibers" *J. Lightwave Techn.* **5**, pp. 1036-1039. 1985
15 NE Fisher, SF O'Neill, DJ Webb, CN Pannell, DA Jackson, LR Gavrilov, JW Hand, L Zhang and I Bennion, "Ultrasonic field and temperature sensor based on short in-fibre Bragg gratings, *Electron. Letts.* **34** pp1139-1140

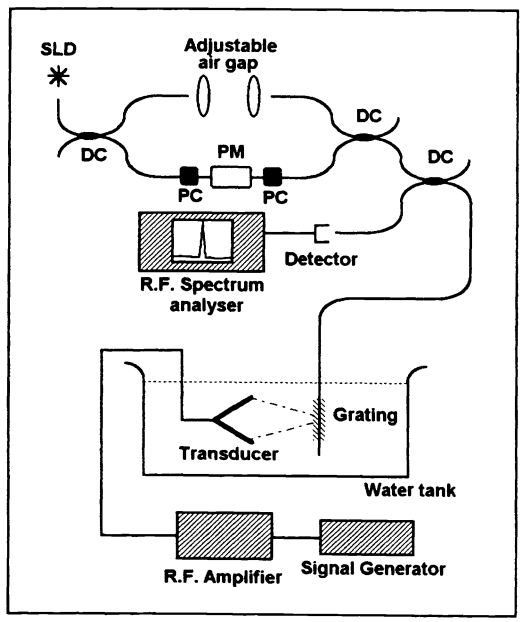

Figure 1. Experimental arrangement
PM = phase modulator
PC = polarisation controller
DC = directional coupler

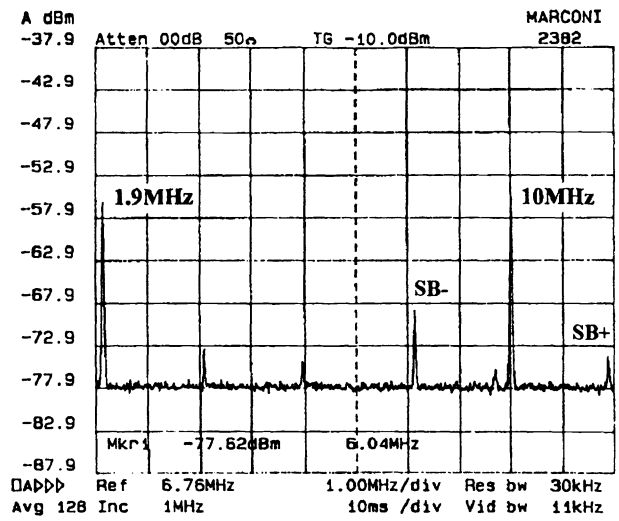

Figure 2. Spectrum analyser trace
SB- = lower frequency side-band
SB+ = upper frequency side-band

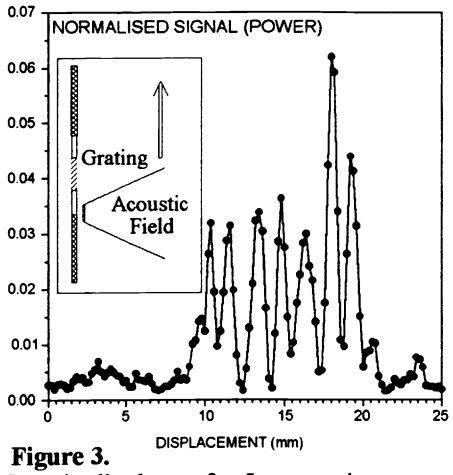

Figure 3.
Longitudinal scan for 5mm grating

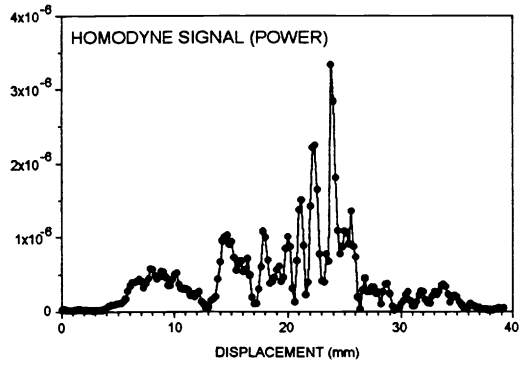

Figure 4. Longitudinal scan for 5mm grating with inter-jacket separation 1cm

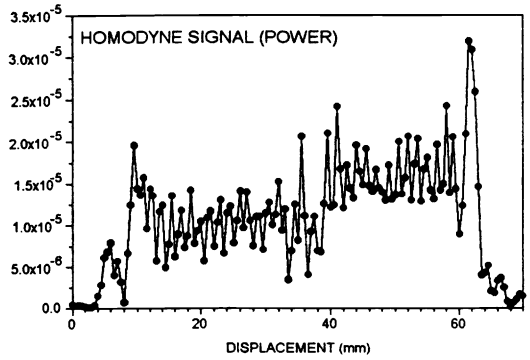

Figure 5. Longitudinal scan for 5mm grating with inter-jacket separation 6cm

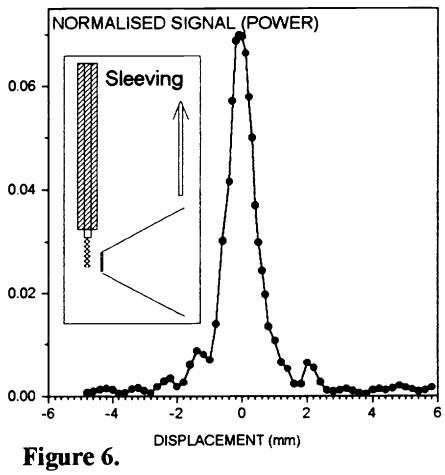

Figure 6.
Longitudinal scan for 1mm grating

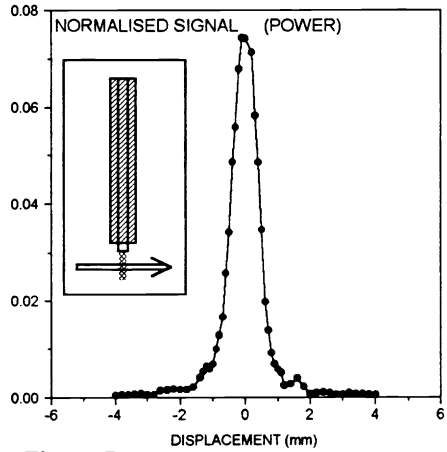

Figure 7.
Transverse scan for 1mm grating

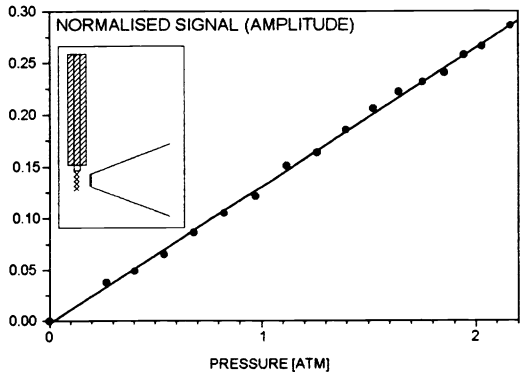

Figure 8. Side-band amplitude (normalised by carrier amplitude) as a function of acoustical pressure incident on 1mm grating.